

Image Demoiréing Using Dual Camera Fusion on Mobile Phones

Yanting Mei, Zhilu Zhang, Xiaohe Wu[†], Wangmeng Zuo

Faculty of Computing, Harbin Institute of Technology, Harbin, China

meiyt0418@gmail.com, cszlzhang@outlook.com, csxhwu@gmail.com, wmuo@hit.edu.cn

Abstract—When shooting electronic screens, moiré patterns usually appear in captured images, which seriously affects the image quality. Existing image demoiréing methods face great challenges in removing large and heavy moiré. To address the issue, we propose to utilize Dual Camera fusion for Image Demoiréing (DCID), *i.e.*, using the ultra-wide-angle (UW) image to assist the moiré removal of wide-angle (W) image. This is inspired by two motivations: (1) the two lenses are commonly equipped with modern smartphones, (2) the UW image generally can provide normal colors and textures when moiré exists in the W image mainly due to their different focal lengths. In particular, we propose an efficient DCID method, where a lightweight UW image encoder is integrated into an existing demoiréing network and a fast two-stage image alignment manner is present. Moreover, we construct a large-scale real-world dataset with diverse mobile phones and monitors, containing about 9,000 samples. Experiments on the dataset show our method performs better than state-of-the-art methods. Code and dataset are available at <https://github.com/Mrduckkk/DCID>.

Index Terms—Image Demoiréing, Dual Camera Fusion, Mobile Phones

I. INTRODUCTION

It has become a common and convenient way to use smartphones to record and transfer data from electronic screens. However, Moiré appears in the captured image, presented as wavy, concentric, and other complex geometric patterns, while it does not exist in the original image. This occurs due to the frequency aliasing phenomenon between the pixel array of the camera sensor and the pixel grid of the displayed screen. Moiré not only affects visual quality, but also may lead to information loss of image textures and details. Therefore, the technique of removing moiré has received widespread attention.

Early moiré removal methods adopt traditional machine learning techniques such as low-rank sparse matrix decomposition [1] and bandpass filtering [2]. With the rise of deep learning, many works design neural networks. For instance, MopNet [3] introduces moiré pattern classification to process them in a divide-and-conquer manner. MBCNN [4] integrates frequency domain modeling. FHDe²Net [5] and ESDNET [6] improve multi-scale processing architecture, experimenting successfully on high-definition and ultra-high-definition (UHD) images, respectively. Although these methods have made great progress in removing light and small

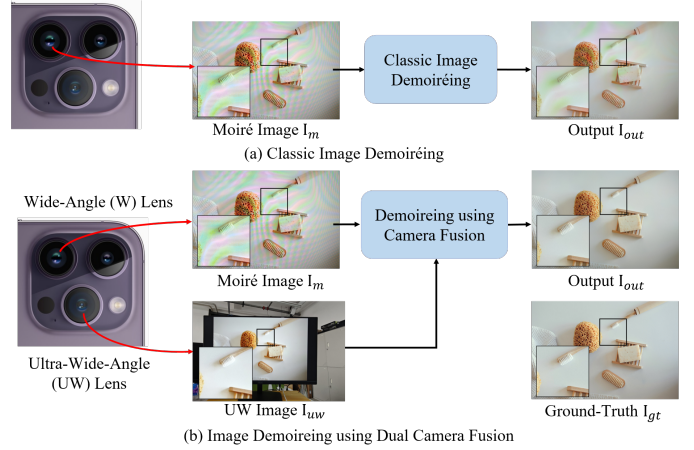


Fig. 1. Comparison of image demoiréing methods. The sub-figure (a) shows a classic image demoiréing with a single input. The sub-figure (b) shows image demoiréing using asymmetric camera fusion.

moiré patterns, they do not have satisfactory performance on severe moiré ones, as shown in Fig. 1 (a). One possible solution is to design a complex and large network to increase model fitting ability. But it would inevitably bring greater computational costs, leading to time-consuming or infeasible inference of UHD images on mobile phones.

To address the issue efficiently, we propose **Dual Camera fusion for Image Demoiréing (DCID)**, *i.e.*, using the ultra-wide-angle (UW) image to assist the moiré removal of wide-angle (W) image. It is based on two motivations. First, modern smartphones are generally equipped with asymmetric multi-lens camera systems, making it possible to collect images from both wide-angle and ultra-wide-angle cameras. Second, from our observation, moiré is sensitive to lens focal length, distance, and angle between the camera and display. W lens serves as the commonly used camera for capturing screen-display contents. When severe frequency aliasing exists between the W sensor and the screen subpixel, the UW image usually does not present obvious moiré patterns, due to the different focal lengths and positions of the UW and W lenses. Thus, the UW image can provide information with low resolution but relatively normal textures and colors, improving the performance for W image demoiréing, as shown in Fig. 1 (b).

In particular, we propose an efficient DCID method. We take a recent single image demoiréing network (*i.e.*, ESDNet [6]) as backbone, and design a lightweight encoder for the UW image. Spatial alignment between UW and W is crucial. Some

[†] Corresponding Author.

This work was supported in part by the National Natural Science Foundation of China (NSFC) under Grant No.62476067, Heilongjiang Science and Technology Project under Grant No.2022ZX01A21.

methods like optical flow [7] and deformable convolution [8] prove ineffective or computationally costly. To resolve this, we propose a fast and efficient two-stage alignment method, first applying alignment on the image level by keypoint matching and then doing that on the feature level by convolution kernel prediction. Finally, the aligned features from UW and W encoders are adaptively fused and fed into the decoder.

Moreover, we construct a large-scale real-world DCID dataset. During the data collection, we focus more on moiré images with messy colors and complex patterns, as this moiré is more difficult to remove and the previous methods generally perform poor ability on it. Using 3 mobile phones to capture 3 displays successively, we obtain about 9,000 samples. During the data pre-processing, we crop the captured UW image and moiré W image as input, and align the source image to the cropped W image as the ground-truth. Moreover, display settings (*e.g.*, brightness, contrast, and color adjustment parameters) make different color tones between the source and captured images, thus, we further align the brightness and color of the source image to the cropped W image ones.

Experiments are conducted on our DCID dataset. The results show that our DCID method achieves better than state-of-the-art image demoiréing methods both in quantitative and qualitative comparison, which demonstrates the effectiveness of the dual camera fusion manner for moiré removal.

Our main contributions can be summarized as follows:

- To improve the effect of severe moiré removal on mobile phones, we propose to utilize **Dual Camera** fusion for **Image Demoiréing** (DCID), where the ultra-wide-angle (UW) image is taken to assist wide-angle (W) image demoiréing.
- We integrate a lightweight UW image encoder into an existing demoiréing network, and propose a fast and efficient two-stage manner to align UW and W images.
- We construct a large-scale real-world DCID dataset with diverse smartphones and monitors, consisting of about 9,000 samples in total.
- Experiments on DCID dataset show our method behaves favorably against state-of-the-art image demoiréing methods both quantitatively and qualitatively.

II. RELATED WORK

A. Image demoiréing

With the rise of mobile photography, moiré patterns have become prevalent, posing significant challenges for image restoration. Traditional demoiréing methods, such as low-rank decomposition [1] and layer decomposition on polyphase components (LDPC) [2], focus on signal processing but incur high computational costs. Deep learning has revolutionized image demoiréing. Early CNN-based approaches, such as MopNet [3] and MBCNN [4], leveraged frequency domain optimization and texture decomposition. Sun *et al.* [9] proposed a multi-scale learning convolutional neural network and the first benchmark dataset captured on LCD screens. Two-stage architectures like FHDe²Net [5] introduced global-to-local

strategies for better texture and color preservation. More recent methods, such as ESDNet [6], focus on lightweight designs for ultra-high-definition image moiré removal. MCFNet [10] proposed a multiscale guided screenshot demoiréing method to understand moiré frequency correlation.

Although significant progress has been made, these methods are limited by the characteristics of the single image itself and cannot remove severe moiré patterns. Considering the current UHD images captured by mobile cameras, we propose to utilize Dual Camera fusion for Image Demoiréing (DCID), where the UW image is taken to assist the W image demoiréing.

B. Reference-based Image Restoration

Reference-based image processing idea is applied in multiple image restoration tasks. For example, RefSR [11]–[13] leverages high-resolution reference images that share similar content and textures to assist the super-resolution of low-resolution input. Zhang *et al.* [14], [15] utilizes blurry long-exposure images to help denoising of sharp short-exposure images. Liu *et al.* [16] introduced a self-adaptive learning method, utilizing an additional defocused moiré-free image to assist in removing moiré patterns from the focused moiré image.

Modern smartphones make UW images easily accessible, and UW images offer richer and detailed information than defocused images. To the best of our knowledge, this work is the first dual-camera fusion method for image demoiréing.

III. DATASET

To achieve DCID, we collect a large-scale real-world dataset using various smartphones and monitors. Below, we detail the dataset construction process.

A. Data Collection

Each sample in the dataset should contain three images, *i.e.*, moiré W images, UW images, and ground-truth (GT). The moiré W and UW images (with less moiré) can be captured using smartphones, where UW images serve as valuable auxiliary information for W image demoiréing. The moiré-free GT image can be obtained from the associated source image displayed on the screen.

Our dataset contains a wide range of common screen display scenarios, including natural scene images, web content, and other materials such as documents and research papers. Moiré patterns with messy colors and intricate geometry significantly affect visual perception and are hard to remove using previous methods. Therefore, we are more concerned with collecting images under these moiré patterns. Moreover, to collect diverse moiré patterns, we capture images with various angles, distances, and lighting conditions, which produce moiré images with a wide array of shapes, scales, and color characteristics.

We use three different brands of smartphones to shoot three different types of displays, which form 9 (3×3) combinations. The detailed configuration is provided in Table I. About 1,000 samples are taken for each combination. Finally, there are 8959 samples in total. The training and test sets consist of 7,176 and

TABLE I
MOBILE PHONE CAMERAS AND DIGITAL SCREENS USED IN OUR DATASET.

Mobile Phone				Digital Screen		
Manufacturer	Model	W Image Size	UW Image Size	Manufacturer	Model	Resolution
HUAWEI	P40	4096 × 3072	4608 × 3456	REDMI	RMMNT238NF	1920 × 1080
Xiaomi	14	4096 × 3072	4080 × 3060	AOC	24B1XH5	1920 × 1080
iPhone	14 Pro	4032 × 3024	4032 × 3024	KTC	H27T13	2560 × 1440

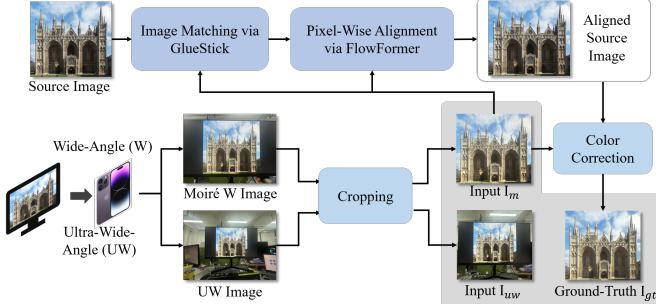


Fig. 2. Data processing pipeline in our DCID dataset.

1,783 samples, respectively. Each combination contains ~ 200 test samples. Compared to existing datasets [5], [6], [9], [17], the images in this dataset exhibit more severe moiré patterns. It significantly increases the difficulty of restoring moiré-free content, providing a challenging benchmark for future works.

B. Data Processing

We first crop the main screen content from the W image, getting the moiré input I_m . Then the UW image is cropped with the same cropping ratio, getting the auxiliary input I_{uw} . To better align I_m and source image I_{gt}^{src} spatially, we perform a two-step image alignment. First, we use Gluestick [18] to perform image matching based on keypoints and keylines, thus roughly aligning the source image to the cropped W image. Next, we further apply a pixel-wise alignment using FlowFormer [7], to align the initially-aligned source image to I_m , getting the finally-aligned source image \tilde{I}_{gt}^{src} .

In existing image demoiréing datasets [5], [6], [9], [17], the brightness and color of GT are generally the same as those of the source image. However, it may not be appropriate, as different display settings (*e.g.*, brightness, contrast, and color adjustment parameters) bring various displayed image appearances. To ensure that the demoiréing method only removes the moiré and does not alter the color representation of the captured image, we perform additional color correction on \tilde{I}_{gt}^{src} . Specifically, a 3×3 color correction matrix is estimated using the least squares method, which represents the linear color mapping between I_m and \tilde{I}_{gt}^{src} . Note that the matrix is calculated between Gaussian blurred I_m and \tilde{I}_{gt}^{src} , which reduces the impact of moiré in I_m and helps to achieve a more accurate color mapping. Finally, we apply the matrix to \tilde{I}_{gt}^{src} , getting the GT I_{gt} . I_{gt} can more faithfully reflect the color state of the scene displayed on the screen.

IV. METHOD

In this section, we introduce our proposed DCID method. We first revisit ESDNet [19]. Then we describe the overall

pipeline of DCID method and detail the two-stage alignment manner. Finally, we give the loss functions.

A. Revisiting ESDNet

ESDNet [19] is a multi-scale encoder-decoder architecture, with a specially designed block at each scale. Each ESDNet [19] block contains a dilated residual dense module and a plug-and-play semantic alignment scale-aware module (SAM). SAM consists of two main modules, *i.e.*, a pyramid feature extraction module and a cross-scale dynamic fusion module, which effectively capture multi-scale features and dynamically integrate image features by learning fusion weights, respectively. These innovations enable ESDNet to achieve superior performance compared to previous works on the LCDmoiré [17], FHDMi [5], and UHDM [6] datasets.

B. Method Overview

When facing complex and irregular moiré patterns, some single image demoiréing methods, *e.g.*, ESDNet, struggle to remove them. To solve this problem, we propose Dual Camera Fusion for Image Demoiréing (DCID), *i.e.*, using the UW image to assist the moiré removal of the W image. UW images, easily captured with smartphones, offer additional information with lower resolution but relatively normal textures, thereby enhancing the performance of W image demoiréing.

The overall architecture of our DCID method is illustrated in Fig. 3. We take ESDNet as the backbone and design a lightweight encoder for the UW image to integrate into it. The lightweight encoder extracts the feature from the UW image, and adopts a simple architecture consisting of three convolutional blocks, each of which contains a downsampling layer and 3-layer convolutions. Compared with ESDNet, this design brings a small amount of additional computational costs.

Then what needs to be done is the alignment and fusion between the UW and W images. Spatial alignment is crucial for getting satisfactory results, but existing alignment manners are generally computationally intensive and time-consuming. In this work, we propose a fast and efficient two-stage alignment method to balance efficiency and performance, which is described in detail in the next subsection. Finally, the aligned features from W and UW encoders are adaptively fused and fed into the decoder.

C. Two-Stage Alignment

The proposed alignment framework consists of two stages, *i.e.*, Keypoint Matching based Alignment (KMA) and Kernel Prediction based Alignment (KPA). The first stage performs

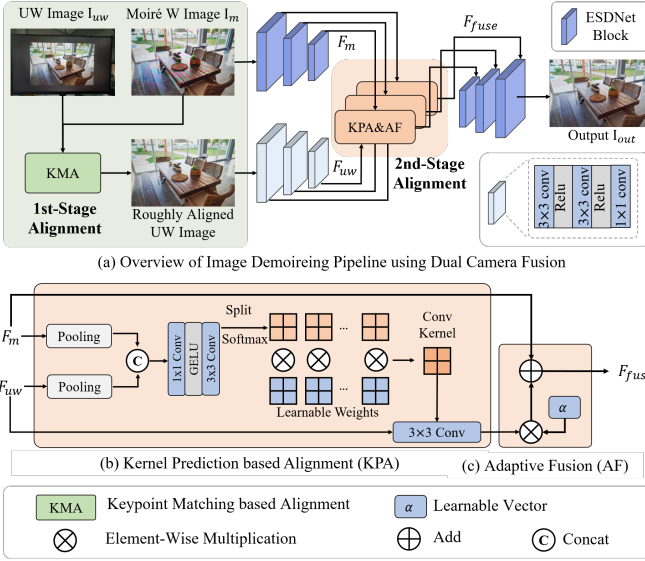


Fig. 3. Pipeline of the proposed DCID method.

coarse geometric alignment on the image level, and the second performs fine-grained alignment on the feature level.

KMA. There is a significant difference in the field of view between UW and W images. In this case, the common optical flow based alignment methods are not cost-effective, *i.e.*, achieving a good alignment performance may come at a high cost. Instead, we propose to perform sparse keypoint matching between the two images, and then utilize the matching prompts to align them. Specifically, we apply SuperPoint [20] to detect 256 keypoints from the $\times 4$ down-sampled images, and then adopt LightGlue [21] to match the keypoints. The keypoints number and down-sampling factor are determined through extensive experiments, and these settings can provide a better trade-off between computational efficiency and alignment performance. Finally, the UW image I_{uw} is roughly aligned to W image I_m according to the keypoint matching results, *i.e.*,

$$\hat{I}_{uw} = \text{KMA}(I_m, I_{uw}), \quad (1)$$

where \hat{I}_{uw} denotes the aligned UW image.

KPA. In the second stage, the KPA module further aligns \hat{I}_{uw} and I_m spatially. We propose to perform that on the multi-scale feature level, as multi-scale features may integrate more fine-grained information and alleviate the adverse impact of moiré on alignment. The W features $F_m \in \mathbb{R}^{C \times H \times W}$ and UW features $F_{uw} \in \mathbb{R}^{C \times H \times W}$ are extracted through their encoders. Applying deformable convolution [8] is a possible choice, but we found that it does not work well here, probably due to unstable optimization. Instead, we estimate transform convolution weights for F_{uw} . TransXNet [22], we construct a KPA module to achieve this. Specifically, adaptive average pooling is first adopted to aggregate contextual information of F_m and F_{uw} , and then they are concatenated along the channel dimension, getting W' , *i.e.*,

$$W' = \text{Concat}(\text{AdaptivePool}(F_m), \text{AdaptivePool}(F_{uw})). \quad (2)$$

Next, two convolutional layers are applied to process W' . To generate the initial convolution kernel weights $W \in$

$\mathbb{R}^{G \times C \times K^2}$ (where G is the number of weight groups and K is the convolution kernel size), we use a softmax function along the group dimensions, *i.e.*,

$$W = \text{Softmax}(\text{Reshape}(\text{Conv}(\text{ReLU}(\text{Conv}(W'))))). \quad (3)$$

By performing element-wise multiplication between W and learnable parameters P , followed by summation along the group dimension, we can obtain a content-adaptive convolution kernel $\theta \in \mathbb{R}^{C \times K \times K}$, *i.e.*,

$$\theta = \sum_{i=0}^G P_i W_i. \quad (4)$$

This kernel is used to transform F_{uw} into \tilde{F}_{uw} , *i.e.*,

$$\tilde{F}_{uw} = \text{Conv}(F_{uw}; \theta). \quad (5)$$

\tilde{F}_{uw} can be regarded as more fine alignment results from \hat{I}_{uw} to I_m .

Finally, the fused feature F_{fuse} is then computed by adaptively combining F_m and \tilde{F}_{uw} using a learnable coefficient $\alpha \in \mathbb{R}^{C \times 1 \times 1}$, α is adaptively learned during training, *i.e.*,

$$F_{fuse} = F_m + \alpha \tilde{F}_{uw}. \quad (6)$$

This fusion strategy effectively integrates information from both W and UW features, ensuring that essential structural and contextual details in W features are preserved.

D. Loss Functions

To enhance the network's capability to remove moiré patterns across multiple scales, we employ a multi-scale loss function. It is applied by a multi-scale supervision mechanism, which constrains the network to learn consistent features across different spatial scales. Moreover, the total loss function integrates ℓ_1 and perceptual loss \mathcal{L}_p terms, which can be written as,

$$\mathcal{L}_{\text{total}} = \sum_{i=1}^3 (\|I_{out}^i - I_{gt}^i\|_1 + \lambda_p \|\phi(I_{out}^i) - \phi(I_{gt}^i)\|_1). \quad (7)$$

where $\phi(\cdot)$ represents the features extracted by the VGG [23] network, λ_p is the weight of perceptual loss, which is set to 2.0, I_{out}^i represents the predicted outputs at scale i , and I_{gt}^i is $\times 2^{i-1}$ downsampled version of the original ground truth I_{gt} .

V. EXPERIMENT

A. Experimental Settings

We evaluate our method on the proposed dataset. To quantitatively assess performance, we employ widely used metrics, including PSNR, SSIM [25], LPIPS [26], and ΔE . PSNR and SSIM are used to measure pixel-wise fidelity and structural similarity, while LPIPS provides a perceptual quality metric aligned with human visual perception. These metrics are widely used in image restoration tasks, including the previous demoiréing works such as ESDNet [6] and MBCNN [4]. ΔE is used to quantify the perceptual color difference between restored and ground-truth images, as chaotic colors often exist

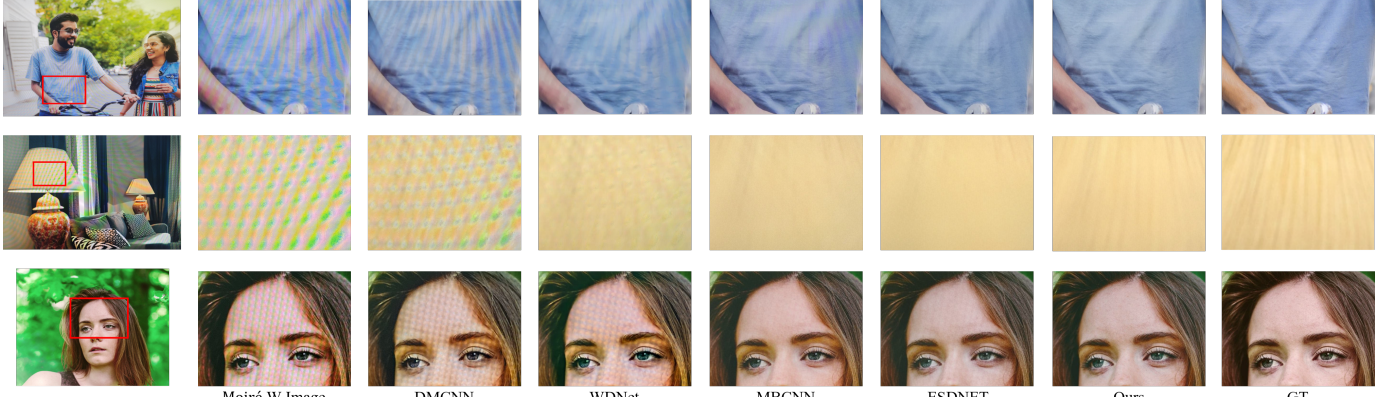


Fig. 4. Visual comparison of demoiréing results among state-of-the-art methods on our dataset. Please zoom in for a better view.

TABLE II

QUANTITATIVE COMPARISONS BETWEEN OUR MODEL AND STATE-OF-THE-ART METHODS ON OUR DATASETS. \uparrow DENOTES THE LARGER THE BETTER, AND \downarrow DENOTES THE SMALLER THE BETTER. METHODS MARKED IN **BOLD** AND UNDERLINED INDICATE THE BEST AND THE SECOND BEST ONE, RESPECTIVELY.

Dataset	Methods	PSNR \uparrow	SSIM \uparrow	LPIPS \downarrow	$\Delta E \downarrow$
Xiaomi	DMCNN [9]	23.36	0.8586	0.314	6.308
	WDNet [24]	25.66	0.8699	0.239	4.670
	MBCNN [4]	25.44	0.8826	0.213	4.496
	<u>ESDNet</u> [6]	<u>26.14</u>	<u>0.8889</u>	<u>0.204</u>	<u>4.166</u>
	Ours	27.06	0.8973	0.197	3.777
HUAWEI	DMCNN [9]	25.12	0.8653	0.338	5.449
	WDNet [24]	26.69	0.8734	0.252	4.383
	MBCNN [4]	26.23	0.8805	0.226	4.339
	<u>ESDNet</u> [6]	<u>27.31</u>	<u>0.8864</u>	<u>0.220</u>	<u>3.892</u>
	Ours	27.72	0.8926	0.212	3.783
iPhone	DMCNN [9]	24.58	0.8617	0.333	5.473
	WDNet [24]	26.08	0.8735	0.259	4.316
	MBCNN [4]	25.97	0.8806	0.242	4.158
	<u>ESDNet</u> [6]	<u>26.36</u>	<u>0.8827</u>	<u>0.232</u>	<u>3.933</u>
	Ours	26.99	0.8831	0.228	3.686

in moiré patterns. This metric is also adopted in the recent image demoiréing method [27].

Our model was implemented using PyTorch on an NVIDIA RTX A6000 GPU. During training, a batch size of 8 is used with 768×768 randomly cropped patches. Initial learning rate 0.0002 follows cyclic cosine annealing [28]. Optimization is performed using the Adam optimizer [29], with $\beta_1 = 0.9$ and $\beta_2 = 0.999$. The model is trained for 500 epochs. For evaluation, the model is tested on full-resolution images without resizing, reflecting real-world application scenarios. To ensure fair evaluation, we also trained competing methods on our dataset using the same configurations.

B. Comparison with the Previous Works

Quantitative Comparison. We compare our method against state-of-the-art approaches, including DMCNN [9], WDNet [24] MBCNN [4], and ESDNet [6]. These methods only input the moiré image. Table II presents the quantitative results on our dataset. Our method achieves state-of-the-art performance, significantly outperforming existing methods across all metrics. Taking the results on the Xiaomi camera dataset as an example, our method improves PSNR by 0.92dB and ΔE by

TABLE III
OTHER METHOD COMPARISONS ON XIAOMI CAMERA DATASET.

Methods	UW	PSNR \uparrow	SSIM \uparrow	LPIPS \downarrow	$\Delta E \downarrow$
RRID [30]	\times	25.47	0.8705	0.233	4.474
UnDeM [31]	\times	23.73	0.8531	0.246	6.046
Ours + RRID [30]	\checkmark	26.01	0.8781	0.214	4.282
Ours + UnDeM [31]	\checkmark	24.51	0.8670	0.222	5.314

0.389 in comparison with ESDNet. It shows the UW image can provide valuable information and help to remove moiré patterns effectively. Additionally, some recent methods do not directly applicable to our dataset. For example, RRID [30] operates on both RAW and RGB images, and UnDeM [31] uses unpaid data for training, while our method focuses on supervised demoiréing on RGB images. To demonstrate the effectiveness of our methods, we adapt them to our settings to conduct experiments. For RRID, we replace the RAW input with RGB image. For UnDeM, we use it to generate pseudo-moiré images and take them to train the demoiréing model. From Table III, our method still outperforms the two methods. Nevertheless, since our method builds upon ESDNet as a baseline, we place particular emphasis on comparing our results with ESDNet.

Qualitative Comparison. Fig. 4 illustrates the visual comparison between our method and existing methods. Our method consistently delivers more perceptually satisfying results. By incorporating UW images, our approach effectively addresses challenges posed by both large-scale and small-scale textures, significantly alleviating the issues caused by moiré patterns. For instance, in the second example in Fig. 4, the textures on the lampshade are obscured by moiré interference in the moiré image, making it hard to restore the details using existing methods. In contrast, with the inclusion of UW images, our method successfully recovers these textures, demonstrating its ability to utilize auxiliary information to enhance the reconstruction of fine contents. This demonstrates the robustness and effectiveness of our proposed method, particularly in processing challenging scenarios.

C. Ablation Study

To validate the effectiveness of our two-stage alignment manner, we conducted ablation studies on the Xiaomi camera

TABLE IV

ABALATION STUDY OF TWO-STAGE IMAGE ALIGNMENT MANNERS ON XIAOMI CAMERA DATASET.

1-Stage	2-Stage	PSNR↑ / SSIM↑ / LPIPS↓ / ΔE↓	#FLOPs (G)	Time (s)
-	-	26.14 / 0.8889 / 0.204 / 4.166	4.478	0.518
OF	-	26.84 / 0.8933 / 0.200 / 3.928	7.698	1.219
KMA	-	26.93 / 0.8936 / 0.198 / 3.882	5.020	0.618
OF	DCN	26.84 / 0.8931 / 0.200 / 3.910	9.940	1.414
KMA	DCN	26.85 / 0.8934 / 0.201 / 3.965	7.262	0.827
OF	KPA	26.94 / 0.8944 / 0.199 / 3.859	7.700	1.250
KMA	KPA	27.06 / 0.8973 / 0.197 / 3.777	5.022	0.659

TABLE V

ABALATION STUDY OF λ_p ON XIAOMI CAMERA DATASET.

λ_p	0	1	2	3	4
PSNR/SSIM	26.06/0.886	27.02/0.895	27.06/0.897	26.55 / 0.893	26.45/0.893
LPIPS/ΔE	0.244/4.184	0.199/3.843	0.197/3.777	0.202/4.035	0.204/4.099

dataset. The first line in Table IV shows the result that the UW image is not used, and we take it as the baseline. First, the single-stage alignment methods, whether based on optical flow (OF) [7] or our KMA, exhibit limited metric improvement, indicating their unsatisfactory image alignment capabilities. In particular, OF doubles the inference time, which is obviously not cost-effective. Second, for the second stage alignment, we compared deformable convolution (DCN) [8] and the proposed KPA module. However, DCN does not bring performance gains, probably due to the difficulty of its optimization. In both OF-based and KMA-based methods, replacing DCN with KPA consistently achieved better PSNR and lower ΔE , highlighting KPA’s efficiency and effectiveness in aligning features and suppressing moiré patterns. Overall, our two-stage alignment (KMA + KPA) design significantly improves the results while only introducing a small increase in computational cost.

We have conducted experiments on the perceptual loss coefficient λ_p . The results in Table V demonstrate that the perceptual loss significantly improves performance. When λ_p is set to 2.0, the model performs best.

VI. CONCLUSION

In this paper, to remove the severe moiré, we propose to perform Dual-Camera fusion for Image Demoiréing (DCID), *i.e.*, leveraging ultra-wide-angle (UW) images to assist wide-angle (W) image demoiréing. To support this, we construct a large-scale real-world DCID dataset with a diverse range of smartphones and monitors. Moreover, the proposed efficient DCID framework integrates a lightweight UW image encoder into the existing demoiréing network and introduces a fast two-stage image alignment manner. Experimental results on the DCID dataset demonstrate that our method significantly outperforms state-of-the-art ones in both quantitative and qualitative evaluations.

REFERENCES

- [1] Fanglei Liu, Jingyu Yang, and Huanjing Yue, “Moiré pattern removal from texture images via low-rank and sparse matrix decomposition,” in *IEEE VCIP*, 2015.
- [2] Jingyu Yang, Fanglei Liu, Huanjing Yue, Xiaomei Fu, Chunping Hou, and Feng Wu, “Textured image demoiréing via signal decomposition and guided filtering,” *IEEE TIP*, 2017.
- [3] Bin He, Ce Wang, Boxin Shi, and Ling-Yu Duan, “Mop moire patterns using mopnet,” in *ICCV*, 2019.
- [4] Bolun Zheng, Shanxin Yuan, Gregory Slabaugh, and Aleš Leonardis, “Image demoiréing with learnable bandpass filters,” in *CVPR*, 2020.
- [5] Bin He, Ce Wang, Boxin Shi, and Ling-Yu Duan, “Fhde 2 net: Full high definition demoiréing network,” in *ECCV*, 2020.
- [6] Xin Yu, Peng Dai, Wenbo Li, Lan Ma, Jiajun Shen, Jia Li, and Xiaojuan Qi, “Towards efficient and scale-robust ultra-high-definition image demoiréing,” in *ECCV*, 2022.
- [7] Zhaoyang Huang, Xiaoyu Shi, Chao Zhang, Qiang Wang, Ka Chun Cheung, Hongwei Qin, Jifeng Dai, and Hongsheng Li, “Flowformer: A transformer architecture for optical flow,” in *ECCV*, 2022.
- [8] Jifeng Dai, Haozhi Qi, Yuwen Xiong, Yi Li, Guodong Zhang, Han Hu, and Yichen Wei, “Deformable convolutional networks,” in *ICCV*, 2017.
- [9] Yujing Sun, Yizhou Yu, and Wenping Wang, “Moiré photo restoration using multiresolution convolutional neural networks,” *IEEE TIP*, 2018.
- [10] Duong Hai Nguyen, Se-Ho Lee, and Chul Lee, “Multiscale coarse-to-fine guided screenshot demoiréing,” *SPL*, 2023.
- [11] Zhilu Zhang, Ruohao Wang, Hongzhi Zhang, Yunjin Chen, and Wangmeng Zuo, “Self-supervised learning for real-world super-resolution from dual zoomed observations,” in *ECCV*, 2022.
- [12] Zhilu Zhang, Ruohao Wang, Hongzhi Zhang, and Wangmeng Zuo, “Self-supervised learning for real-world super-resolution from dual and multiple zoomed observations,” *IEEE TPAMI*, 2024.
- [13] Gyunmin Shim, Jinsun Park, and In So Kweon, “Robust reference-based super-resolution with similarity-aware deformable convolution,” in *CVPR*, 2020.
- [14] Zhilu Zhang, RongJian Xu, Ming Liu, Zifei Yan, and Wangmeng Zuo, “Self-supervised image restoration with blurry and noisy pairs,” *NeurIPS*, 2022.
- [15] Zhilu Zhang, Shuhao Zhang, Renlong Wu, Zifei Yan, and Wangmeng Zuo, “Bracketing is all you need: Unifying image restoration and enhancement tasks with multi-exposure images,” *ICLR*, 2025.
- [16] Lin Liu, Shanxin Yuan, Jianzhuang Liu, Liping Bao, Gregory Slabaugh, and Qi Tian, “Self-adaptively learning to demoiré from focused and defocused image pairs,” *NeurIPS*, 2020.
- [17] Shanxin Yuan, Radu Timofte, Gregory Slabaugh, and Aleš Leonardis, “Aim 2019 challenge on image demoiréing: Dataset and study,” in *ICCV Workshops*, 2019.
- [18] Rémi Pautrat, Iago Suárez, Yifan Yu, Marc Pollefeys, and Viktor Larsson, “Gluestick: Robust image matching by sticking points and lines together,” in *ICCV*, 2023.
- [19] Yulun Zhang, Yapeng Tian, Yu Kong, Bineng Zhong, and Yun Fu, “Residual dense network for image super-resolution,” in *CVPR*, 2018.
- [20] Daniel DeTone, Tomasz Malisiewicz, and Andrew Rabinovich, “Supernet: Self-supervised interest point detection and description,” in *CVPR Workshops*, 2018.
- [21] Philipp Lindenberger, Paul-Edouard Sarlin, and Marc Pollefeys, “Light-glue: Local feature matching at light speed,” in *ICCV*, 2023.
- [22] Meng Lou, Hong-Yu Zhou, Sibei Yang, and Yizhou Yu, “Transxnet: learning both global and local dynamics with a dual dynamic token mixer for visual recognition,” *IEEE TNNLS*, 2025.
- [23] K Simonyan and A Zisserman, “Very deep convolutional networks for large-scale image recognition,” in *ICLR*, 2015.
- [24] Lin Liu, Jianzhuang Liu, Shanxin Yuan, Gregory Slabaugh, Aleš Leonardis, Wengang Zhou, and Qi Tian, “Wavelet-based dual-branch network for image demoiréing,” in *ECCV*, 2020.
- [25] Zhou Wang, Alan C Bovik, Hamid R Sheikh, and Eero P Simoncelli, “Image quality assessment: from error visibility to structural similarity,” *IEEE TIP*, 2004.
- [26] Richard Zhang, Phillip Isola, Alexei A Efros, Eli Shechtman, and Oliver Wang, “The unreasonable effectiveness of deep features as a perceptual metric,” in *CVPR*, 2018.
- [27] Yuxin Zhang, Mingbao Lin, Xunchao Li, Han Liu, Guozhi Wang, Fei Chao, Shuai Ren, Yafei Wen, Xiaoxin Chen, and Rongrong Ji, “Real-time image demoiréing on mobile devices,” *ICLR*, 2023.
- [28] Ilya Loshchilov and Frank Hutter, “Sgdr: Stochastic gradient descent with warm restarts,” *ICLR*, 2017.
- [29] Diederik P Kingma, “Adam: A method for stochastic optimization,” *ICLR*, 2015.
- [30] Shuning Xu, Binbin Song, Xiangyu Chen, Xina Liu, and Jiantao Zhou, “Image demoiréing in raw and srgb domains,” in *ECCV*, 2024.
- [31] Yunshan Zhong, Yuyao Zhou, Yuxin Zhang, Fei Chao, and Rongrong Ji, “Learning image demoiréing from unpaired real data,” in *AAAI*, 2024.